



# Bulletin of the Mineral Research and Exploration

<http://bulletin.mta.gov.tr>



## Assessment of soil liquefaction using the energy approach

Kamil KAYABALI<sup>a\*</sup>, Pınar YILMAZ<sup>b</sup>, Mustafa FENER<sup>c</sup>, Özgür AKTÜRK<sup>d</sup> and Farhad HABIBZADEH<sup>e</sup>

<sup>a</sup>Ankara University Geological Engineering Department, Gölbaşı, Ankara, Türkiye orcid.org/0000-0002-0228-0777

<sup>b</sup>General Directorate of Mineral Research and Exploration, Department of Feasibility Study, Ankara, Türkiye orcid.org/0000-0002-2749-8924

<sup>c</sup>Ankara University Geological Engineering Department, Ankara 06100, Türkiye orcid.org/0000-0003-0491-3205

<sup>d</sup>Akdeniz University Geological Engineering Department, Antalya, 07038, Türkiye orcid.org/0000-0001-7703-5779

<sup>e</sup>Ankara University Geological Engineering Department, Ankara 06100, Türkiye orcid.org/0000-0001-5672-5834.

Research Article

### Keywords:

Liquefaction, stress method, strain method, energy method, earthquake energy.

### ABSTRACT

Damage to structures during earthquakes may be fully or partly caused by soil liquefaction, which has been the subject of extensive research for several decades. Liquefaction susceptibility of a sandy deposit is performed by comparing the resistance of a soil to liquefaction (i.e., capacity) to the load imparted by an earthquake (i.e., demand). In this regard, the stress-based method of liquefaction assessment is by far the most popular. It involves uncertainties mostly related to the computation of the maximum horizontal ground acceleration ( $a_{max}$ ) at bedrock. A site response analysis or a simplified assumption is necessary to determine the  $a_{max}$  on the ground level as well. Developing from the stress-based approach, the strain-based approach has also similar constraints. There exist laboratory techniques such as torsional shear to determine the capacity of a sandy soil in terms of liquefaction energy per unit volume. Likewise, the energy of a strong motion record can be set by employing simple physics principles. For this, a velocity time history and the unit mass of the soil are employed to compute the demand of any strong motion record. The scope of this investigation is to illustrate the usability of the energy-based method for the evaluation of soil liquefaction. The deficiencies of the stress- and strain-based approaches are outlined and the advantages of the energy-based approach are discussed.

Received Date: 01.08.2017

Accepted Date: 28.09.2017

## 1. Introduction

Loose sand undergoes densification, which entails an increase in pore water pressure, when subjected to ground shaking or other type of cyclic loading. When the excess pore pressure equals the effective stress, the phenomenon known as liquefaction takes place. The liquefaction of saturated loose sands during strong ground motion is a major cause of damage and catastrophic failure in buildings, embankments, and other civil engineering structures. The most spectacular manifestations of ground failure due to soil liquefaction were observed during the 1964 Niigata, 1989 Loma Prieta, and 1999 Chi-Chi earthquakes.

Because many factors influence the mechanism of liquefaction, the assessment of the liquefaction

potential of cohesionless soils is a complex engineering problem. Such factors include the magnitude and intensity of an earthquake, the seismic attenuation characteristics, the distance from the hypocenter, propagation path effects, soil type and properties, confining pressure, the geometry of soil layers, and other site-specific conditions (Law et al., 1990).

Extensive liquefaction research has been performed over the last few decades. Numerous researchers have investigated the liquefaction potential of sands using laboratory methods (DeAlba et al., 1976; Ladd et al., 1989), field methods (Davis and Berrill, 2001; Çetin et al., 2004), and numerical techniques (Chen et al., 2005; Baziar and Jafarian, 2007; Zhang et al., 2015; Kokusho et al., 2015; Kokusho and Mimori, 2015).

\* Corresponding author: Kamil KAYABALI, [kayabali@ankara.edu.tr](mailto:kayabali@ankara.edu.tr)  
<http://dx.doi.org/10.19111/bulletinofmre.351257>

Several procedures have been developed to evaluate the liquefaction potential of cohesionless soils in the field. The evaluation tools can be categorized into three main groups: 1) Stress-based procedures, 2) strain-based procedures, and 3) energy-based procedures (Green, 2001; Zhang et al., 2015). By far, the stress-based approach (Seed and Idriss, 1971) is the most commonly employed technique for liquefaction evaluation in the field.

The scope of this investigation is to outline the basic principles of the three approaches on soil liquefaction, to bring forward the deficiencies of the stress-based and strain-based procedures, and to propose the energy-based approach as a new and practical tool for the assessment of soil liquefaction in the field in accordance with further improvements.

## 2. Background on Soil Liquefaction Evaluation Methods

Soil liquefaction evaluation techniques unambiguously attempt to determine two factors: The first is the strength of the soil against the occurrence of liquefaction, or its “capacity.” The second is the load imparted to the soil by the earthquake, or the “demand” (Green, 2001; Alavi and Gandomi, 2012). The factor of safety against liquefaction is defined as the ratio of capacity to demand.

### 2.1 The Stress-Based Method

By far the most commonly employed method for liquefaction evaluation is the stress-based method (Seed and Idriss, 1971; Whitman, 1971). It is often based on empirical data from field observations and laboratory investigations, and has been continually updated (Youd et al., 2001; Çetin et al., 2004) as new contributions have come in from ongoing research.

Demand in the stress-based approach based on the Seed simplified method is the amplitude of the load imparted by the earthquake, defined as the cyclic stress ratio (CSR):

$$CSR = \frac{\tau_{ave}}{\sigma'_o} = 0.65 \frac{a_{max}}{g} \frac{\sigma_o}{\sigma'_o} r_d \quad (1)$$

where CSR = cyclic stress ratio,  $\tau_{ave}$  = average shear stress imposed by the strong ground motion,  $a_{max}$  = maximum horizontal acceleration on the ground surface, g = gravitational acceleration,  $\sigma'_o$  = initial effective vertical stress at depth z,  $\sigma_o$  = total vertical stress at depth z, and  $r_d$  = dimensionless stress

reduction factor. The quantity of  $r_d$  varies with depth and an average value is computed by the following relationship (NCEER, 1997):

$$r_d = \frac{(1.0 - 0.4113z^{0.5} + 0.04052z + 0.001753z^{1.5})}{(1.0 - 0.4117z^{0.5} + 0.05729z - 0.006205z^{1.5} + 0.00121z^2)} \quad (2)$$

Equation (1) is valid only for M = 7.5 earthquakes. Seismic events other than M = 7.5 are taken into account by introducing a “magnitude scaling factor” (MSF), for which a number of empirical forms have been proposed by different researchers. The most recent version of MSF relationships is given by Idriss and Boulanger (2006) as follows:

$$\text{MSF} = 6.9 \exp(-0.25M) - 0.058 \quad (3)$$

(valid when MSF  $\leq 1.8$ )

The CSR for earthquakes other than M = 7.5 is obtained by dividing the result of Equation (1) by the MSF obtained from Equation (3).

The resistance of cohesionless soils to liquefaction, or capacity, is usually expressed by the standard penetration resistance of  $(N_1)_{60}$ , which stands for a standard penetration test (SPT) blow count based on a hammer impact efficiency of 60% and an overburden pressure of 1 atm. It should be noted that  $(N_1)_{60}$  is for clean sands; it should be modified to take into account fines content (FC) to obtain an equivalent clean sand value,  $(N_1)_{60cs}$ , as follows (Youd et al., 2001):

$$(N_1)_{60cs} = (N_1)_{60} + \exp \left[ 1.63 + \frac{9.7}{FC+0.1} - \left( \frac{15.7}{FC+0.1} \right)^2 \right] \quad (4)$$

For the stress-based approach, Seed and Idriss (1971) proposed 65% of maximum shear stress for 15 cycles of applied cyclic load. Ishihara and Yasuda (1972, 1975), using a pattern of time histories of shear stress scaled from the recorded strong ground motions of the Niigata earthquake, found that equivalent shear stress was 57% of maximum shear stress, rather than the 65% proposed by Seed and Idriss (1971). Accordingly, the Seed simplified approach overpredicts the average shear stress imparted by the earthquake by some 12%.

One other important issue to be addressed is the maximum horizontal ground acceleration,  $a_{max}$ , on the ground surface. Once the epicentral distance from the causative fault or the earthquake source to the project site and the magnitude of the earthquake are known, the maximum horizontal ground acceleration for bedrock can be computed by using an appropriate strong motion attenuation relationship. The use of

proper values for both the magnitude and the distance is of utmost importance; yet, the magnitude, the type of distance to be used (e.g., epicentral distance, hypocentral distance, or distance to the causative fault), and even the attenuation relationship itself inherits some degrees of uncertainties. Computation of the maximum horizontal ground acceleration on the ground surface involves a site response analysis, which requires a detailed set of information such as small-strain shear wave velocity profile, thickness, strain compatible modulus/damping curves and total density of soil layers with regard to the soil profile at a project site. It is a costly procedure and commonly carried out for significant engineering structures (i.e., power plants, high-rise buildings, etc.). The alternative to the determination of  $a_{max}$  on the ground surface through a site response analysis is the use of a simplified approach employing charts such as those given by Seed and Idriss (1982), which provides only an approximation for  $a_{max}$  on the ground surface of overly simplified soil profiles, such as shallow sand soils, deep cohesive soils, and alike. A site response analysis might end up with a significantly "amplified" strong motion, which, in turn, results in a higher CSR. The amplification factor in Seed and Idriss (1982) is only for a non-liquefied ground and does not account for soil nonlinearity in the liquefied soil. That's among the reasons for over estimation of the  $a_{max}$  at the surface.

Acceleration is a vector, and ground acceleration has three components. The stress-based approach considers only the higher of two horizontal  $a_{max}$  values; some researchers argue that the vertical component should also be taken into account (Atkinson, 1986; Law et al., 1990).

## 2.2. The Strain-Based Method

This procedure is based on the hypothesis that pore pressure begins to develop when shear strain reaches the threshold value. It was first proposed by Dobry et al. (1982). It was derived from the mechanics of two interacting idealized sand grains and then generalized for natural soil deposits (Green, 2001; Baziar and Jafarian, 2007; Alavi and Gandomi, 2012). The amplitude of the earthquake-induced cyclic shear strain, or demand, is determined by following relationship:

$$\gamma = \frac{0.65 \frac{a_{max}}{g} \sigma_{ord}}{G_{max} \left( \frac{G}{G_{max}} \right)_y} \quad (5)$$

where  $G_{max}$  = shear modulus corresponding to  $\gamma = 10^{-4}\%$ ,  $G/G_{max}$  = ratio of shear moduli corresponding to  $\gamma$  and  $\gamma = 10^{-4}\%$  (Green, 2001). The other variables are the same as those for Equation (1). Upon a series of strain-controlled cyclic tests on saturated undrained clean sand specimens, Dobry et al. (1982) showed that the capacity, or the threshold shear strain ( $\gamma_{th}$ ), for liquefaction to initiate is approximately 0.11%.

Practical difficulties pertinent to determining the variables of Equation (5) mainly include ascertaining  $G_{max}$  and ratio of shear moduli. For the former, either in situ tests (e.g., a downhole test, a crosshole test, etc.) or complex empirical forms are required. For the latter, each soil has its own characteristic of shear modulus degradation. Laboratory determination of the ratio of shear moduli as a function of shear strain is cumbersome. Although a number of shear modulus degradation curves have been published, they provide only an approximation for the targeted threshold shear strain for a specific type of soil.

The alternative use of the strain-based procedure involves the concept of the total strain energy required for the onset of liquefaction as obtained either from laboratory experiments or records of strong ground motion. A typical cyclic load test provides stress, strain, and pore pressure data. Hysteresis loops of shear stress-strain as a function of time such as the one shown in figure 1 is obtained. The strain energy

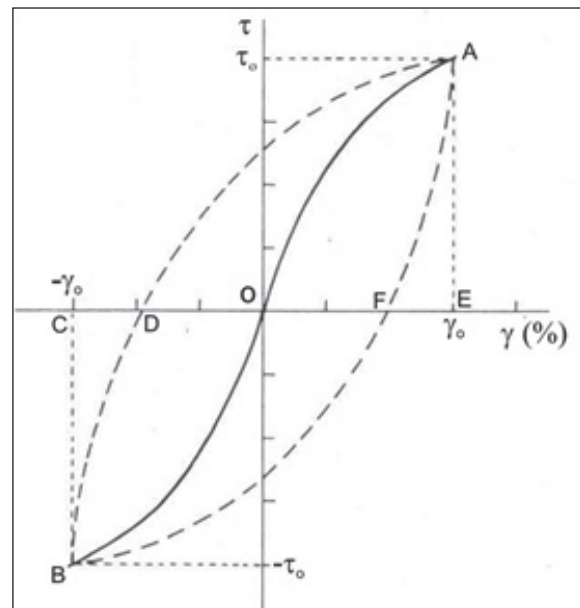


Figure 1- A typical shear stress-strain hysteresis loop (modified from Hardin and Drenich, 1972).

for each cycle of loading is equivalent to the area inside the hysteresis loop of BDAFB in figure 1 (Ostadian, 1996; Green, 2001; Zhang et al., 2015). The instantaneous energy and its summation over time intervals are computed until the onset of liquefaction. The summation of the energy at this time is used as the measure of the capacity of the soil specimen against liquefaction (Alavi and Gandomi, 2012). This observation has prompted the formulation of the energy-based approach, details of which are presented in the following sub-section.

Although the strain-based approach is theoretically reasonable, it is less popular than the stress-based procedure due to the fact that the strain approach only estimates the initiation of pore pressure buildup, which is essential for liquefaction to occur, but does not necessarily imply that liquefaction will occur. The main deficiency of this method is the greater difficulty of estimating cyclic shear strain compared with cyclic shear stress (Seed, 1980; Zhang et al., 2015).

### 2.3. The Energy-Based Method

The concept of energy in the analysis of densification and liquefaction of sands was first introduced by Nemat-Nasser and Shokoh (1979). The energy, which is associated with the permanent rearrangement of sand particles, under a certain set of conditions leading to liquefaction, is a constant quantity. The accumulated energy per unit volume ( $J/m^3$ ) associated with the permanent rearrangement of particles is given by the area inside the hysteresis loop developed during a cycle (Figure 1). The accumulated energy per unit volume ( $\delta W$ ) absorbed by the specimen until it liquefies is given as follows (Figueroa et al., 1994; Liang et al., 1995):

$$\delta W = \sum_{i=1}^{n-1} \frac{1}{2} (\tau_i + \tau_{i+1})(\gamma_{i+1} - \gamma_i) \quad (6)$$

where  $\tau$  = shear stress,  $\gamma$  = shear strain and  $n$  = number of cycles recorded to liquefaction.

To predict liquefaction, the strain energy to initiate liquefaction is compared with the strain energy imparted by earthquake to the sand layer during the seismic design event. The experiments revealed that the build-up of the excess pore pressure is proportional to the total strain energy in all loading cycles up to the initial liquefaction (Alavi and Gandomi, 2012). David and Berrill (2001) conducted a study for field verification of pore pressure and dissipated energy during earthquakes and concluded that the dissipated

energy density may be remarkably well correlated with pore pressure increases in field conditions.

Figueroa et al. (1994) conducted a series of tests on Reid Bedford sand using a hollow-cylinder torsional shear device. They established a relationship between the dissipated energy per unit volume imparted to the soil to reach liquefaction and parameters such as effective confining pressure, relative density, and amplitude of shear strain:

$$\log(W) = 2.002 + 0.00477\sigma'_{mean} + 0.0116D_r \quad (7)$$

where  $W$  = measured strain energy density required for triggering liquefaction ( $J/m^3$ ),  $\sigma'_{mean}$  = initial effective mean confining pressure (kPa), and  $D_r$  = initial relative density (%).

A few of similar relationships compiled by Alavi and Gandomi (2012) are as follows:

$$\log(W) = 2.062 + 0.0039\sigma'_{mean} + 0.0124D_r \quad (\text{Liang, 1995}) \quad (8)$$

$$\log(W) = 1.164 + 0.0124\sigma'_{mean} + 0.0209D_r \quad (\text{Dief and Figueroa, 2001}) \quad (9)$$

$$\log(W) = 2.1028 + 0.004566\sigma'_{mean} + 0.005685D_r + 0.001821FC - 0.02868C_u + 2.0214D_{50} \quad (\text{Baziar and Jafarian, 2007}) \quad (10)$$

where  $FC$  = percentage of fines content,  $C_u$  = coefficient of uniformity, and  $D_{50}$  = mean grain size (mm). The most recent empirical expression relating the measured strain energy ( $W$ ; in  $kJ/m^3$ ) for liquefaction to the initial mean stress ( $\sigma'$  in kPa), and relative density ( $D_r$ ; in decimals), was provided by Jafarian et al. (2012):

$$W = 0.1363P'_o(D_r^{4.925}) + 5.375(10^{-3}P'_o) \quad (11)$$

The main advantages of the energy-based method over the stress-based and strain-based approaches are that: 1) the energy is a scalar quantity expressed by a single number; 2) it is not necessary to decompose the time history of shear stress to find an equivalent cycle number for selected average stress or strain level; and 3) its use encompasses both stress and strain, as well as material properties (Law et al., 1990; Liang et al., 1995). For the field case, soils amplify the ground motion in certain frequency ranges. They do attenuate it in other frequency ranges. This implies that, whether part of the motion is amplified or attenuated, the total

energy traveling through and dissipated in a soil remains unchanged (Law et al., 1990).

### 3. The Proposed Method

It is possible to compute the quantity of energy, E (in Joules), released during an earthquake. The total energy released from an earthquake is given by (Gutenberg and Richter, 1956):

$$E = 10^{4.8} + 1.5M \quad (12)$$

where M is the magnitude on the Richter scale (Law et al., 1990). Some of this energy is dissipated by inelastic attenuation along ray paths, and further attenuation occurs due to geometric spreading (Davis and Berrill, 1982). Only a very small fraction of this energy arrives at any site. The following procedure explains how the energy imparted by an earthquake on a unit of mass is computed.

The work imparted on a system (W) is explained as follows (anonymous physics rule):

$$W = 0.5mV^2 \quad (13)$$

where m is mass and V is velocity. For practical purposes, the system is defined as 1 m<sup>3</sup> of soil. To determine the work imparted by an earthquake on a unit volume of soil, a strong motion record such as an acceleration-time history is needed. This acceleration time history is simply integrated with respect to time to transform it into a velocity-time history. Once the mass of unit soil (it is actually absolute value of the saturated density since the volume is 1 unit) is known, it is used directly in a spreadsheet program to obtain either the work-time history or cumulative work versus the time. Figures 2 and 3 show the acceleration and velocity time histories for the September 20,

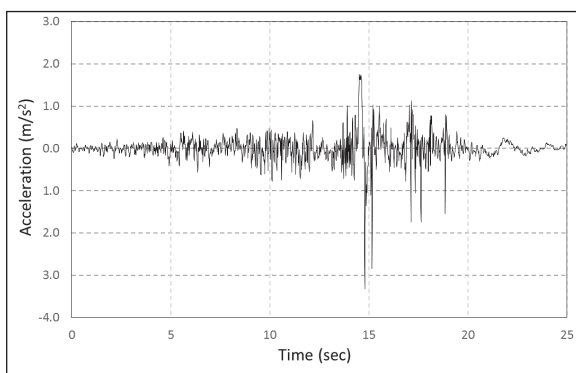


Figure 2- N-S accelerogram of the 1999 Chi-Chi earthquake recorded at Taichung (Miaoli-Shitan School), Taiwan.

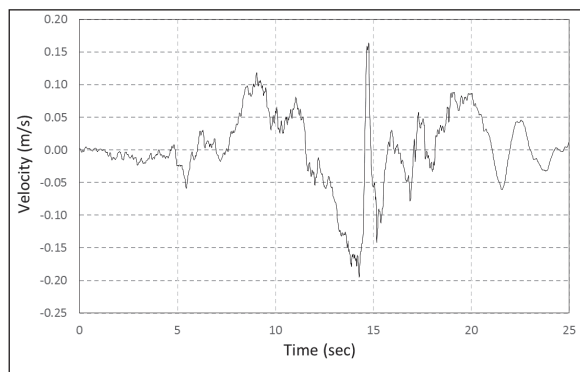


Figure 3- The velocity time history for the Taichung (Miaoli-Shitan School), Taiwan acceleration record.

1999, Chi-Chi, Taiwan, earthquake ( $M_w = 7.6$ ) recorded at Taichung, Taiwan (station No.: TCU045). The work time history of the event is computed for a saturated soil with a density of 2000 kg/m<sup>3</sup> (Figure 4). Figure 5 includes the cumulative energy for the same event. As figure 5 implies, the total work imparted on 1 cubic meter of soil, for which the mass is 2000 kg, during an event lasting 40 seconds is 7.9 kJ. For

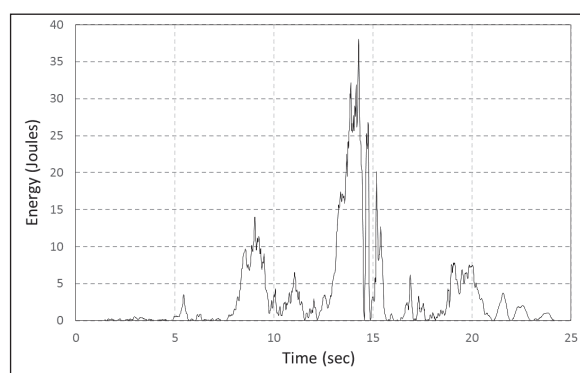


Figure 4- The work time history for the Taichung (Miaoli-Shitan School), Taiwan acceleration record.

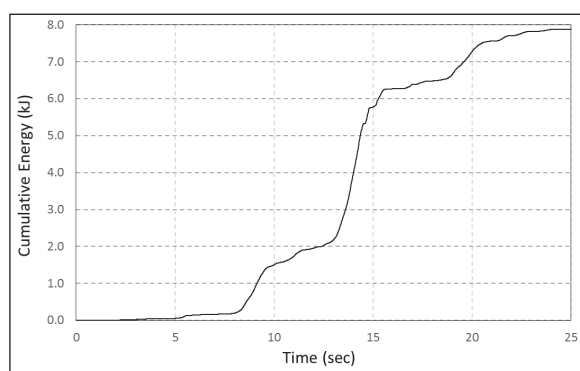


Figure 5- The cumulative energy plot for the Taichung (Miaoli-Shitan School), Taiwan acceleration record.

practical considerations, only the significant portion of the 90-second record is taken. In other words, the beginning and the ending parts of the acceleration record that do not contribute significantly to the cumulative energy are simply omitted. Removal of such portions of the record can be done by a simple spread-sheet operation.

The next step after the procedure for computing the energy of a specific record of strong ground motion involves determining the soil parameters.

The strain energy equations formulated through Equations 7–11 all involve the use of the initial effective mean confining pressure,  $\sigma'_{mean}$ . The difficulty of determining  $\sigma'_{mean}$  in situ should be appreciated. In field conditions, the initial effective overburden stress ( $\sigma'_v$ ) is commonly used as the representative of effective shear strength rather than the initial mean effective stress,  $\sigma'_{mean}$  or  $P'_o$ , which could be interchangeably related as (Seed et al., 1986):

$$\sigma'_{ort} = \left( \frac{1+2K_o}{3} \right) \sigma'_v \quad (14)$$

where  $K_o$  = coefficient of lateral earth pressure at rest. It is defined by the following generic form as:

$$K_o = 1 - \sin(\phi') \quad (15)$$

The effective angle of internal friction,  $\phi'$ , in Equation (15) can be determined as (Hatanaka and Uchida, 1996):

$$\phi' = (20N_{1,60})^{0.5} + 20 \quad (16)$$

Finally, the relative density is defined as follows (Skempton, 1986):

$$D_r = 15(N_{1,60})^{0.5} \quad (17)$$

The characterization of soil parameters to be used in determining “capacity” is carried out by the following order:

- i) The corrected blow count ( $N_{1,60}$ ) is determined from the standard penetration test (considering the uncertainties with the standard penetration test, an alternative and more reliable way of obtaining relative density directly can be done by employing the cone penetration test)
- ii) The effective initial vertical stress ( $\sigma'_{vo}$ ) is computed using the field data

- iii)  $\phi'$  is determined from Equation (16)
- iv)  $K_o$  is computed from Equation (15)
- v)  $K_o$  and  $\sigma'_{vo}$  are plugged into Equation (14) to get  $\sigma'_{mean}$
- vi) Equation (17) is employed to compute the relative density for clean sands; Equation (4) is employed to find the “equivalent” relative density for fine-grained soils
- vii) The capacity of a soil against liquefaction is computed using any of the Equations 7–11.

Once the mean effective stress and the relative density are at hand, the energy required to liquefy the soil concerned can easily be computed. The total unit mass,  $M_t$ , is then employed to obtain the energy imparted by the earthquake on 1 m<sup>3</sup> of saturated soil. The final step is only a comparison between the capacity and demand.

To provide an idea of the typical energy applied on a cubic meter of soil at any point in the vertical soil profile, table 1 was constructed. The saturated density was assumed as 2000 kg/m<sup>3</sup> for all calculations. Table 1 includes some significant events in the world along with some characteristics of near-source records of strong ground motion.

To show how the energy imparted by an earthquake onto a cubic meter volume of soil changes with distance and site conditions, table 2 was prepared using strong motion records obtained during the October 18, 1989, Loma Prieta event. The saturated density was assumed the same as before. All strong motion data used for the construction of tables 1 and 2 came from the Pacific Earthquake Engineering Research Center.

To demonstrate how the proposed method works table 3 was constructed which covers 4 field cases; the two of them experienced liquefaction and the two did not during the Loma Prieta event. The partial data in table 3, namely  $a_{max}$ , depths to layer of interest and water table, the total and effective vertical stresses on the layer, ( $N_{1,60}$ ), fines content and ( $N_{1,60cs}$ ) were taken from Idriss and Boulanger (2010).  $\gamma_{sat}$  and  $M_t$  were deduced from the imported data using the depth to water table, the total stress and the effective stress in the same data source.  $\sigma'_{mean}$ ,  $K_o$ ,  $\phi'$  and  $D_r$  were computed using the equations of 14–17. The capacities ( $W_{liq}$ ) were calculated for 4 different empirical

Table 1- Some characteristics of significant events in the world along with their energy imparted onto one cubic meter of soil ( $M_w$ : moment magnitude;  $a_{max}$ : maximum horizontal ground acceleration; R: distance to causative fault; W: total work done; \*:  $M_L$ ).

Event	$M_w$	Station No.	$a_{max}$ (g)	R (km)	W (kJ/m <sup>3</sup> )
Chi-Chi Taiwan Sep. 20, 1999	7.6	TCU045	0.34	25	7.9
Hollister (USA) April 9, 1961	5.6*	USGS1028	0.18	21	3.0
Imperial Valley (USA) Oct. 15, 1979	6.5	USGS5115	0.37	16	3.0
Kobe (Japan) Jan. 16, 1995	6.9	CUE90	0.34	22	17
Kocaeli (Turkey) August 17, 1999	7.4	KOERI330	0.32	23	103
Landers (USA) June 28, 1992	7.3	SCE24	0.73	2.0	12.4
Loma Prieta (USA) Oct. 18, 1989	7.0	CDMG47381	0.37	6.3	18.4
Northridge (USA) Jan. 17, 1994	6.7	CDMG24278	0.58	24	21.1

Table 2- Computed cumulative works for the strong motion records of the 1989 Loma Prieta earthquake obtained from different parts of California, USA.

Location	Station No.	R (km)	$a_{max}$ (g)	Site geology	W (kJ/m <sup>3</sup> )
Capitola	CMG47125	16	0.47	Alluvium/Building	14.4
Hollister	CMG47189	25	0.07	Rock/Free field	3.73
Fremont	CMG57064	35	0.10	Alluvium/Building	2.41
Hayward	CMG58219	45	0.08	Rock/Building	1.76
San Francisco	CMG58539	53	0.10	Rock/Free field	0.74
Piedmont	CMG58338	64	0.08	Rock/Free field	1.37
Point Bonita	CMG58042	73	0.07	Rock/Building	2.21
Larkspur	USGS1590	85	0.14	Marsh/Building	7.71
Olema	CMG68003	107	0.16	Alluvium/Building	4.04

relationships (Equations 7, 8, 9 and 11) by employing the appropriate mean effective stresses and the relative densities.

For the computation of demands the strong ground motion records nearest to the site of interest were selected. Figure 6 shows the time histories of acceleration, velocity and the cumulative work for the 2 cases. The first site of liquefaction (Case #1) is the Treasure Island (site geology: alluvium). There exists a seismic recording station in Treasure Island. For this field the unit mass for the soil was taken as 1800 kg which resulted in a demand of 5200 J/m<sup>3</sup> (Figure 6) when the equation 13 was used along with the velocity time history of the Treasure Island. Since the

demand for the Treasure Island record is greater than the soil capacities calculated using the 4 predictive equations the liquefaction at this site is verified from the viewpoint of the proposed method. The Case #2 is for a site which did not liquefy during the Loma Prieta event. This site is located at Moss Landing, San Francisco and the nearest recording site is located in Salinas, San Francisco (site geology: fill). The demand for this site is calculated as 2200 J/m<sup>3</sup> (Figure 6) using the unit mass of 1900 kg which is smaller than the capacities computed using the predictive equations of Dief and Figueroa (2001) and Jafarian et al. (2012). This finding is also in agreement with the framework of the proposed method; however, Figueroa et al. (1994) and Liang (1995) predictive equations resulted in

Table 3- Computed liquefaction energies and earthquake energies for 4 different cases ( $\gamma_{\text{sat}}$  = unit weight,  $M_i$  = mass of the soil for the volume of 1 m<sup>3</sup>,  $W_{\text{liq}}$  = energy required for liquefaction,  $W_{\text{quake}}$  = energy imposed by the earthquake over soil. Data from Idriss and Boulanger, 2010).

	Case #1	Case #2	Case #3	Case #4
<b>Earthquake and site</b>	<b>Loma Prieta Treasure Island</b>	<b>Loma Prieta Sandboldt UC-B10</b>	<b>Loma Prieta Sandboldt UC-B10</b>	<b>Loma Prieta Alameda Bay Farm Dike</b>
$M_w$	6.9	6.9	6.9	6.9
$a_{\max}$ (g)	0.16	0.28	0.28	0.24
Liquefaction ?	Yes	No	Yes	No
Depth to layer (m)	6.5	6.1	3.0	6.5
Depth to water table (m)	1.5	1.8	1.8	3.0
$\sigma_v$ (kPa) (kPa)	116	115	55	125
$\sigma'_v$ (kPa) (kPa)	67	73	43	91
$(N_i)_{60}$	6.4	34.4	15.3	43.3
Fines content (%)	20	5	2	7
$(N_i)_{60cs}$	10.8	34.4	15.3	43.4
$\gamma_{\text{sat}}$ (kN/m <sup>3</sup> )	18.0	19.0	18.0	19.5
$M_i$ (kg)	1800	1900	1900	1950
$\phi'$ (°)	31.3	46.2	37.5	49.4
$K_o$	0.48	0.28	0.39	0.24
$\sigma'_{\text{mean}}$ (kPa)	44	38	26	45
$D_r$ (%)	49	88	59	99
$W_{\text{liq}}$ (J/m <sup>3</sup> )	Figueroa et al. (1994)	606	1596	638
	Liang (1995)	698	1998	775
	Dief and Figueroa (2001)	546	2966	509
	Jafarian et. al., (2012)	236	2949	389
$W_{\text{quake}}$ (J/m <sup>3</sup> )		5200	2200	2200
				5600

smaller capacities than the demand. The third location (Case #3) is a site of liquefaction in Moss Landing as well. The unit mass of soil at this site is also 1900 kg and thus the cumulative work or the demand is the same as that for Case #2, namely 2200 J/m<sup>3</sup>, which is greater than all the capacities calculated using the 4 predictive equations which supports the hypothesis presented in this investigation. The last location (Case #4) is Alameda Bay Farm Dike in San Francisco. No liquefaction was observed at this site during the event of Loma Prieta. The nearest recording site is at the Treasure Island. The unit mass of 1950 kg for this site along with the equation 13 and the velocity time history of Treasure Island (Figure 6) resulted in a cumulative work or demand of 5600 J/m<sup>3</sup>, for which

the two of the equations predicted no-liquefaction and the two of them predicted liquefaction as for the Case #2.

The comparison between the capacities and demands using the limited number of case studies suggests that the proposed method has a premise to be used in soil liquefaction analysis. While the demands computed using the unit mass and a velocity time history is somewhat unambiguous, the computation of capacities is likely to cover some degrees of uncertainties. The failure of the proposed method to predict soil liquefaction using the two of the predictive equations may be attributed to such uncertainties.

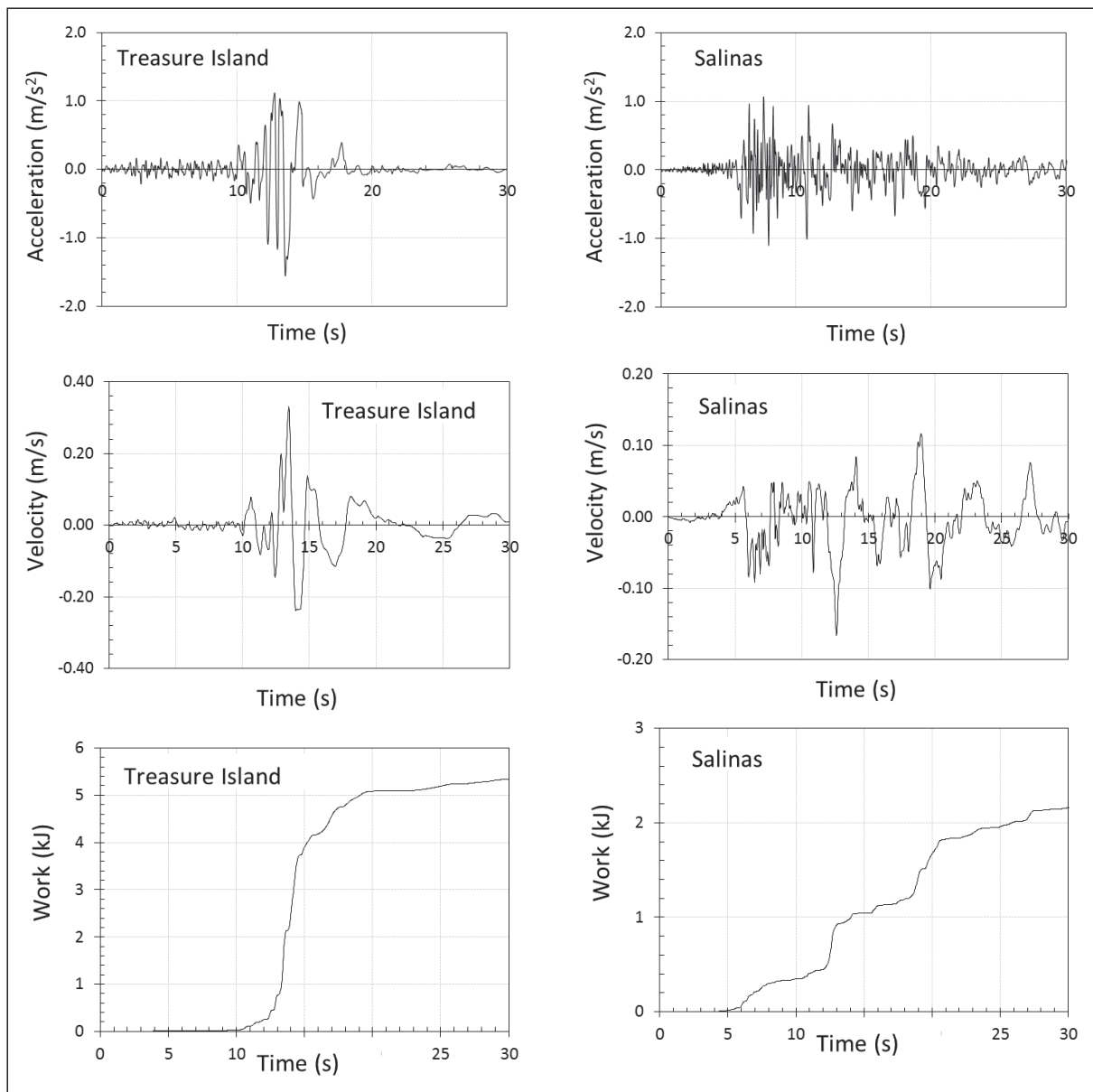


Figure 6- Example time histories of acceleration, velocity and cumulative work for the cases examined.

#### 4. Discussion and Conclusions

The present study resulted in the following conclusions:

The resistance of a sandy deposit against liquefaction can be determined in terms of energy per unit volume. Based upon a series of laboratory tests, some researchers have established empirical relationships allowing the computation of liquefaction energy by employing simple soil parameters such as the relative density and the effective mean confining stress at the layer of interest.

The energy level of a seismic event at any site can be simply determined by the kinetic energy formula. The unit mass of a saturated soil is employed in the formula along with the velocity time history to obtain the total energy of the strong motion record.

The susceptibility of a sandy deposit for liquefaction can be easily checked by a number of strong motion records encompassing a large range of magnitudes and varying distances, using the concept of "earthquake energy."

The stress- and strain-based procedures to determine demand require  $a_{max}$  on the ground level as the major input. Due to uncertainties of attenuation relationships the computation of  $a_{max}$  could be significantly speculative. Moreover, a site response analysis or an oversimplified assumption is to be made to convert  $a_{max}$  at bedrock level to  $a_{max}$  on the ground level. Because the total energy traveling through and being dissipated in a soil remains unchanged, neither  $a_{max}$  at bedrock level nor a site response analysis for  $a_{max}$  on the ground level is needed for the energy-based procedure. This is probably the most distinctive superiority of the energy-based approach over the other two methods of liquefaction assessment.

Both the stress-based and the strain-based procedures to compute demand involve the use of an average shear stress value of 65%. Some researchers argue that this value is conservative. The computation of the energy of a strong motion record does not involve such a correction procedure.

Both the stress- and strain-based approaches also involve a depth correction factor,  $r_d$ , and the proposed method does not need this approximation either.

The results presented herein are based solely on the limited number of case studies. A great number of case analyses is needed in order for the energy-based method to be used in soil liquefaction analyses reliably. There is an ongoing research on the subject matter by the authors covering worldwide data.

## References

- Alavi, A.H., Gandomi, A.H. 2012. Energy-based numerical models for assessment of soil liquefaction. *Geoscience Frontiers* 3(4), 541-555.
- Atkinson, G. M. 1986. Ground motion for eastern North America. Ontario Hydro, Toronto, Ont., Report, 86353.
- Baziar, M.H., Jafarian, Y. 2007. Assessment of liquefaction triggering using strain energy concept and ANN model, capacity energy. *Soil Dynamics and Earthquake Engineering*, 27, 1056–1072.
- Chen Y. R., Hsieh, S. C., Chen, J. W., Shih, C. C. 2005. Energy-based probabilistic evaluation of soil liquefaction, *Soil Dynamics and Earthquake Engineering* 25(1):55-68.
- Davis, R.O., Berrill, J.B. 1982. Energy dissipation and seismic liquefaction in sands. *Earthquake Engineering and Structural Dynamics*, 10, 59-68.
- Cetin, K.O., Seed, R.B., Der-Kiureghian, A., Tokimatsu, K., Harder, Jr. L.F., Kayen, R.E., Moss, R.E.S. 2004. Standard penetration test-based probabilistic and deterministic assessment of seismic soil liquefaction potential. *Journal of Geotechnical and Geoenvironmental Engineering*, ASCE 130(12), 1314–1340.
- Davis, R.O., Berrill, J.B. 2001. Pore pressure and dissipated energy in earthquakes-Field verification. *Journal of Geotechnical and Geoenvironmental Engineering*, ASCE, 127(3), 269-274.
- DeAlba, P.S., Seed, H.B. Chan, C.K. 1976. Sand liquefaction in large-scale simple shear tests. *Journal of Geotechnical Engineering Division ASCE*, 102(GT9): 909–927.
- Dief, H.M., Figueroa, J.L. 2001. Liquefaction assessment by the energy method through centrifuge modeling. In: Zeng, X.W. (Ed.), *Proceedings of the NSF International Workshop on Earthquake Simulation in Geotechnical Engineering*. CWRU, Cleveland, OH.
- Dobry, R., Ladd, R., Yokel, F., Chung, R., Powell, D. 1982. Prediction of pore water pressure buildup and liquefaction of sands during earthquakes by the cyclic strain method. National Bureau of Standards Building Science Series, US Dept of Commerce, 138 p.
- Figueroa, J.L., Saada, A.S., Liang, L., Dahisaria, M.N. 1994. Evaluation of soil liquefaction by energy principles. *Journal of Geotechnical Engineering*, ASCE, 120(9): 1554–1569.
- Green, R.A. 2001. Energy-based evaluation and remediation of liquefiable soils. PhD dissertation, Virginia Polytechnic Institute and State University, Blacksburg, VA.
- Gutenberg, B. Richter, C.F. 1956. Earthquake magnitude, intensity and acceleration. *Bulletin of the Seismological Society of America*, 46, 104-105.
- Hardin, B.O., Drnevich, V.P. 1972. Shear modulus and damping in soils – design and curves. *ASCE Journal of the Soil Mechanics and Foundations Division*, 94 (SM3), 689-708.
- Hatanaka M., Uchida A. 1996. Empirical Correlation between Penetration Resistance and Internal Friction Angle of Sandy Soils. *Soils and Foundations*, 36(4): 1-9.
- Idriss, I.M., Boulanger, R.W. 2006. Semi-empirical procedures for evaluating liquefaction potential during earthquakes. *Soil Dynamics and Earthquake Engineering*, 26, 115-130.

- Idriss, I.M., Boulanger, R.W. 2010. SPT-based liquefaction triggering procedures. Report No. UCD/CGM-10-02, Center for Geotechnical Modeling Department, University of California Davis, California, USA, 136 pp.
- Ishihara, K., Yasuda, S. 1972. Sand liquefaction due to irregular excitation. *Soils and Foundations*, 12(4), 65-77.
- Ishihara, K., Yasuda, S. 1975. Soil liquefaction in hollow cylinder torsion under irregular excitation. *Soils and Foundations*, 15(1), 45-59.
- Jafarian, Y., Towhata, I., Baziar, M.H., Noorzad, A., Bahmanpour, A. 2012. Strain energy based evaluation of liquefaction and residual pore water pressure in sands using cyclic torsional shear experiments. *Soil Dynamics and Earthquake Engineering*, 35, 13-28.
- Kokusho T., Mimori, Y. 2015. Liquefaction potential evaluations by energy-based method and stress-based method for various ground motions, *Soil Dynamics and Earthquake Engineering*, 75, 130-146.
- Kokusho T., Mimori, Y., Kaneko, Y., 2015. Energy-based liquefaction potential evaluation and its application to a case history, 8th Int. Conf. on Earthquake Geotechnical Engineering, New Zealand.
- Kokusho, T., Mimori, Y., Kaneko, Y., 2015, Energy-Based Liquefaction Potential Evaluation and its Application to a Case History: 6th Int'l. Conf. Earthquake Geotechnical Engineering, 1-4 November 2015, Christchuech, New Zealand.
- Ladd, R.S., Dobry, R., Yokel, F.Y., Chung, R.M. 1989. Pore water pressure buildup in clean sands because of cyclic straining. *ASTM Geotechnical Testing Journal*, 12(1), 2208-2228.
- Law, K.T., Cao, Y.L., He, G.N. 1990. An energy approach for assessing seismic liquefaction potential. *Canadian Geotechnical Journal*, 27, 320-329.
- Liang, L. 1995. Development of an energy method for evaluating the liquefaction potential of a soil deposit. PhD dissertation, Department of Civil Engineering, Case Western Reserve University, Cleveland, OH.
- Liang, L., Figueroa, J.L., Saada, A.S. 1995. Liquefaction under random loading: a unit energy approach. *Journal of Geotechnical Engineering*, ASCE 121(11). 776-781.
- NCEER, 1997. Proceeding of the NCEER Workshop on Evaluation of Liquefaction Resistance of Soils. T. L. Youd and I. M. Idriss, eds., Technical Report NCEER-97-0022, National Center for Earthquake Engineering Research, State University of New York, Buffalo, 276 pp.
- Nemat-Nasser S., Shokooh, A.A. 1979. Unified approach to densification and liquefaction of cohesionless sand in cyclic shearing. *Can Geotech J* 1979; 16(4), 659-678.
- Ostadian, F., Deng, N., Arango, I. 1996. Energy-based method for liquefaction potential evaluation - Phase I, feasibility study. U.S. Department of Commerce, Technology Administration, National Institute of Standards and Technology, Building and Fire Research Laboratory.
- Seed, H.B. 1980. Closure to soil liquefaction and cyclic mobility evaluation for level ground during earthquakes. *J. Geotech. Eng. ASCE* 106 (GT6), 724.
- Seed, H.B., Idriss, I.M. 1971. Simplified procedure for evaluating soil liquefaction potential. *J Soil Mech Found Div., ASCE*, 97 (SM8): 1249-1274.
- Seed, H.B., Idriss, I.M. 1982. Ground motions and soil liquefaction during earthquakes. Monograph Series, Earthquake Engineering Research Institute, Oakland, CA, 134 p.
- Seed, H.B., Wong, R.T., Idriss, I.M., Tokimatsu, K. 1986. Moduli and damping factors for dynamic analyses of cohesionless soils. *Journal of Geotechnical Engineering*, 112(GT11), 1016-1032.
- Skempton, A.W. 1986. Standard penetration test procedures and the effects in sand of overburden pressure, relative density, particle size, aging, and overconsolidation. *Geotechnique*, 21, 305-321.
- Whitman, R.V. 1971. Resistance of soil to liquefaction and settlement. *Soils and Foundations*, 11(4), 59-68.
- Youd, T.L., Idriss, I.M., Andrus, R.D., Arango, I., Castro, G., Christian, J.T., Dobry, R., Finn, W.D.L., Harder, L.F., Hynes, M.E., Ishihara, K., Koester, J.P., Liao, S.S.C., Marcuson, W.F., Martin, G.R., Mitchell, J.K., Moriawaki, Y., Power, M.S., Robertson, P.K., Seed, R.B., Stokoe, K.H. 2001. Liquefaction resistance of soils - Summary report from the 1996 NCEER and 1998 NCEER/NSF workshops on evaluation of liquefaction resistance of soils. *Journal of Geotechnical and Geoenvironmental Engineering* 127(4), 817-833.
- Zhang W, Goh A.T.C., Zhang, Y., Chen, Y., Xiao, Y. 2015. Assessment of soil liquefaction based on capacity energy concept and multivariate adaptive regression splines: *Engineering Geology*, 188, 29-37.

